Selective albuminuria via podocyte albumin transport in puromycin nephrotic rats is attenuated by an inhibitor of NADPH oxidase

Satoshi Kinugasa[1], Akihiro Tojo[1], Tatsuo Sakai[2], Harukuni Tsumura[3], Masafumi Takahashi[4], Yasunobu Hirata[1] and Toshiro Fujita[1]

[1]*Department of Internal Medicine, University of Tokyo, Tokyo, Japan;* [2]*Department of Anatomy and Life Structure, Juntendo University School of Medicine, Tokyo, Japan;* [3]*Biomedical Department, Sankei Corporation, Tokyo, Japan and* [4]*Division of Bioimaging Sciences, Center for Molecular Medicine, Jichi Medical University, Tochigi, Japan*

The mechanism of selective albuminuria in minimal change nephrotic syndrome, in which glomerular capillaries are diffusely covered by effaced podocyte foot processes with reduced slit diaphragms, is unknown. Podocyte injury is due, in part, to NADPH-induced oxidative stress. Here we studied mechanism of selective albuminuria in puromycin aminonucleoside (PAN) nephrotic rats, a model of minimal change nephrotic syndrome. In these rats, Evans Blue-labeled human albumin was taken up by podocytes and its urinary excretion markedly increased, with retained selectivity for albumin. Immunogold scanning electron micrographic images found increased human albumin in podocyte vesicles and on the apical membrane in nephrotic compared with control rats. Apocynin, an inhibitor of NADPH oxidase, decreased superoxide production in podocytes, and inhibited endocytosis and urinary albumin excretion. Real-time confocal microscopy found an initial delay in the appearance of Evans Blue-labeled human albumin in the tubular lumen, reflecting the time needed for transcellular transport. Immunoprecipitation analysis indicated that FcRn, a receptor for albumin transport, mediated podocyte albumin transport, and treatment with anti-FcRn antibody reduced proteinuria in these nephrotic rats. Thus, podocyte albumin transport was enhanced in PAN nephrotic rats by means of FcRn, which may explain the mechanism of selective proteinuria. This was blocked by apocynin, suggesting a new therapeutic approach.

Kidney International (2011) **80,** 1328–1338; doi:10.1038/ki.2011.282; published online 17 August 2011

KEYWORDS: glomerular filtration barrier; NADPH oxidase; nephrotic syndrome; podocyte; reactive oxygen species

Correspondence: *Akihiro Tojo, Division of Nephrology and Endocrinology, Department of Internal Medicine, University of Tokyo, 7-3-1 Hongo, Bunkyo-ku, Tokyo 11-8655, Japan. E-mail: akitojo-tky@umin.ac.jp*

Received 15 March 2011; revised 31 May 2011; accepted 14 June 2011; published online 17 August 2011

The mechanism of proteinuria in minimal change nephrotic syndrome (MCNS) remains a mystery. In particular, it is unclear why such large amounts of protein can leak from the glomerular capillaries, which are diffusely covered by effaced foot processes, and how selectivity for albumin is retained when slit pores are assumed to be morphologically damaged because of reduced nephrin expression.

It is generally accepted today that the slit diaphragm is the main filtration barrier for proteins, whereas the glomerular basement membrane (GBM) is a coarse pre-filter.[1] However, in the past, there has been considerable controversy over which component of the glomerulus is the most important barrier, since the slit diaphragm was identified in 1955.[2] Farquhar *et al.*[3,4] stated it was the GBM, based on studies using ferritin and dextran, for these tracers accumulated on the luminal surface of the GBM, but not under the slit diaphragm. The 'GBM theory' was also supported by the concept of the charge barrier.[5] Recently, laminin-β2-deficient mice were shown to develop proteinuria, creating renewed interest in the GBM.[6] By contrast, Karnovsky *et al.*[7] proposed the 'slit diaphragm theory' in a study demonstrating the 'zipper structure' with slit pores identical in size to albumin. He also conducted tracer studies with horseradish peroxidase (HRP), myeloperoxidase, and catalase, and found immunohistochemical staining at the slit diaphragm.[8,9] Identification of slit diaphragm proteins such as nephrin, the mutations of which cause proteinuria, has further strengthened this theory.[10,11] Thus, today it is generally believed that protein molecules are filtered through the slit diaphragm, and in nephrotic states, protein is assumed to leak from enlarged slit pores because of decreased nephrin expression.

However, in MCNS, podocyte slits are markedly reduced with a tight junction-like alteration,[12] and we did not observe glomerular albumin filtered through the slit diaphragm using 8 nm gold- or fluorescein isothiocyanate-labeled albumin in puromycin aminonucleoside (PAN) nephrosis, a representative MCNS model.[13] The limitations of the study were that free fluorescein isothiocyanate cannot be completely removed

even after intensive dialysis, and thus may have influenced the results, and that 8 nm gold-labeled albumin is too large to pass through the slit pores. To solve these limitations, in the present study we used human serum albumin labeled with Evans Blue (EB), which strongly and specifically binds to albumin without altering the molecular weight or shape of albumin due to its small size (961 kDa).[14] We have attempted to visualize three dimensionally the glomerular transport pathways of EB-labeled human serum albumin in a rat MCNS model using immunogold scanning electron microscope (SEM), and also investigated the time course of albumin transport using green fluorescent protein (GFP) transgenic rats. Moreover, as oxidative stress via NADPH oxidase is involved in podocyte injury,[15] we have verified the effects of its inhibitor, apocynin, on podocyte albumin handling. As a mechanism of selective albuminuria in MCNS, we hypothesized the existence of specific receptors for albumin transport in podocytes, and we tested antibodies against FcRn, which is one of the receptors for albumin transport.[16,17]

RESULTS

Podocyte uptake and urinary excretion of EB-labeled human serum albumin

First, we tried to visualize glomerular albumin transport by using EB-labeled human serum albumin as a tracer, which is detectable by both light and fluorescence microscopy, and quantifiable by spectrophotometry. EB specifically binds to albumin, with minimal free EB ($<0.001\%$) in the supernatant after precipitation by trichloroacetic acid. We also verified by gel electrophoresis that EB does not alter the charge of albumin, for the migration distance by charge was identical between EB-labeled human serum albumin and unlabeled albumin, which has an isoelectric point of 4.9.[18] Light micrographs after 90 min of EB-labeled human serum albumin injection showed that EB-labeled albumin uptake was markedly increased in both glomerular cells and proximal tubule cells in PAN nephrotic rats, whereas it was absent in glomeruli with slight uptake in proximal tubule cells in controls (Figure 1a and b). Confocal microscopic observation of EB fluorescence also confirmed increased EB-labeled albumin uptake by these cells in PAN nephrosis, but not in the control (Figure 1c and d). Podocyte uptake showed some heterogeneity among podocytes. Western blotting using microdissected glomeruli showed that glomerular uptake of EB-labeled human serum albumin was increased in PAN rats (Figure 2b). In accordance with these findings, clearance studies showed a 132-fold increase in 24 h urinary EB-labeled human serum albumin excretion in PAN nephrotic rats compared with controls (Figure 2a). SDS-PAGE of urine confirmed that proteinuria was highly selective for albumin (Figure 2c and d).

Albumin passage through the glomerulus visualized by immunogold TEM and SEM

By observation at subcellular levels with immunogold transmission electron microscopy (TEM) and SEM, we found numerous gold particles labeling human serum albumin located inside cytoplasmic vesicles in images of podocyte cross-sections in PAN rats (Figures 3b and 4d), whereas they scarcely existed in podocytes of controls (Figures 3a and 4c), suggesting increased podocyte endocytosis in PAN nephrosis. Immunogold TEM images also showed gold particles, indicating human albumin localized on apical membranous protrusions and microvilli (Figure 3c and d), and albumin-including vesicles just about to be excreted from the apical membrane (Figure 3e). SEM observation confirmed these results, and gold particles labeling human serum albumin on the surface of podocytes were increased in PAN nephrotic rats compared with controls (Figure 4a and b). Moreover, observation at higher magnification in the secondary electron mode revealed multiple granular protrusions on the podocyte surface, suggesting shedding vesicles in PAN nephrosis (Figure 4e and f). These results suggested that albumin passes through the podocyte cell body and is excreted into the urinary space in nephrotic conditions.

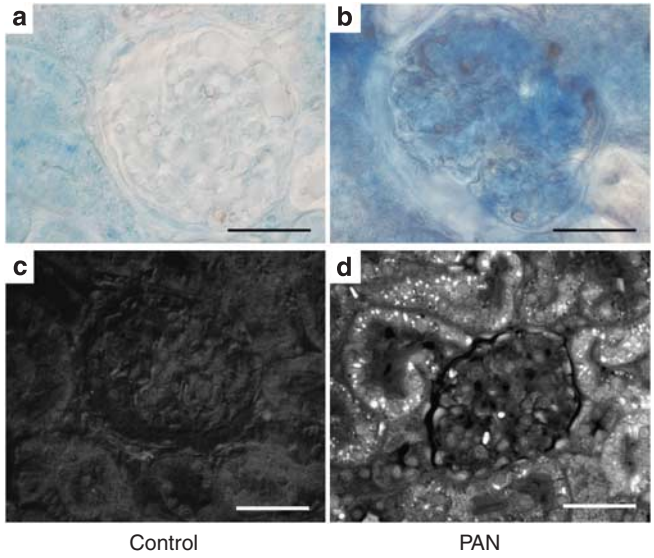

Figure 1 | Renal uptake of injected Evans Blue (EB)-labeled human serum albumin is increased in puromycin aminonucleoside (PAN) nephrotic rats. Images of kidneys after continuous injection for 90 min in controls (**a**, **c**) and PAN nephrotic rats (**b**, **d**). (**a**, **b**) Light micrographs of vibratome sections of rat kidneys. (**c**, **d**) Confocal images showing localization of EB-labeled human serum albumin in 5 μm Lowicryl sections. Uptake of EB-labeled human serum albumin was markedly increased in podocytes and proximal tubular cells. The degree of uptake was heterogenous among podocytes. Bar = 50 μm.

Increased reactive oxygen species production in podocytes in PAN nephrosis

Reactive oxygen species (ROS) produced by NADPH oxidase are presumed to cause podocyte injury in PAN nephrosis. We detected the NADPH oxidase component p47phox staining on the podocyte plasma membrane and cytoplasmic vesicles by immunocytochemistry in PAN rats, but not in controls (Figure 5a). Superoxide production detected by

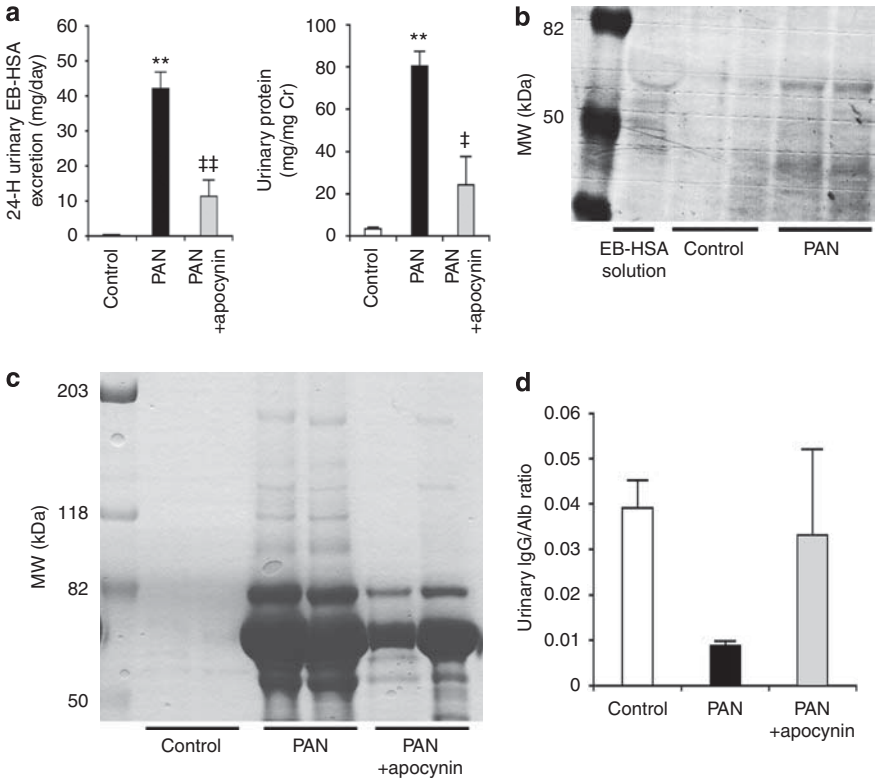

Figure 2 | Twenty-four hours renal clearance study after a single injection of Evans Blue-labeled human serum albumin (EB-HSA) in controls, nephrotic rats induced by puromycin aminonuculeoside (PAN) at 5 days, and PAN rats treated with apocynin starting 2 days before PAN injection (PAN + apocynin). (**a**) Measurement of 24 h urinary EB-labeled human serum albumin excretion and proteinuria. Data are shown as mean ± s.e.m. $^{**}P < 0.01$ versus control. $^{‡}P < 0.05$, $^{‡‡}P < 0.01$ versus PAN. (**b**) Western blotting for human serum albumin of microdissected glomeruli. Uptake of albumin by glomerular cells was increased in PAN nephrotic rats. (**c**) SDS-PAGE for urine. (**d**) Densitometry was performed to calculate the urinary IgG/albumin ratio, in order to compare the selectivity of urinary proteins. Each group includes five rats. Cr, creatinine.

cerium chloride histochemistry was observed on the plasma membrane of podocytes, the GBM, and endothelial cells on day 2 after PAN injection, whereas it was almost negative in controls (Figure 5c). Urinary H_2O_2 excretion peaked on day 2, preceding proteinuria or foot process effacement, and returned to baseline at day 7 when proteinuria peaked with full-fledged foot process effacement (Figure 5b).

The effect of NADPH oxidase inhibition by apocynin on podocyte albumin transport

We examined the effects of NADPH oxidase inhibition by apocynin, derived from the medicinal herb *Picrorhiza kurroa*, and found that apocynin treatment significantly suppressed urinary H_2O_2 excretion, 24 h urinary EB-labeled human serum albumin excretion, and proteinuria in PAN nephrotic rats (Figures 2a and 5b). Foot process effacement was partly restored with apocynin treatment (Figure 6b), and immunogold particles for EB-labeled human serum albumin in podocyte vesicles, cytoplasm, and cell surface in PAN nephrotic rats were significantly decreased with apocynin treatment (Figure 6), suggesting that apocynin inhibits albumin endocytosis and shedding excretion.

In vivo real-time observation of EB-labeled human serum albumin in GFP transgenic rats

To elucidate the time course of glomerular albumin transport, we observed kidneys of GFP transgenic rats after EB-labeled human serum albumin injection with real-time confocal microscopy. The red fluorescence of EB was absent in the proximal tubular lumen until 5 min after injection, and increased at 15 min in PAN rats, whereas it was almost negative in controls (Figure 7a), indicating that a large proportion of albumin is slowly transported through podocytes. In vibratome sections of kidney, the cytoplasm of some podocytes appeared yellow in PAN nephrotic rats, due to merging of the green fluorescent signals of GFP and the red fluorescence of EB, which was not observed in controls (Figure 7b). The degree of EB-labeled human serum albumin uptake by podocytes was heterogenous among cells. These results further reinforced the hypothesis that albumin is transported through the podocyte cytoplasm.

The role of FcRn in albumin transportation

As FcRn has been reported as an albumin and immunoglobulin (Ig)G receptor known to be expressed on podocytes,[16]

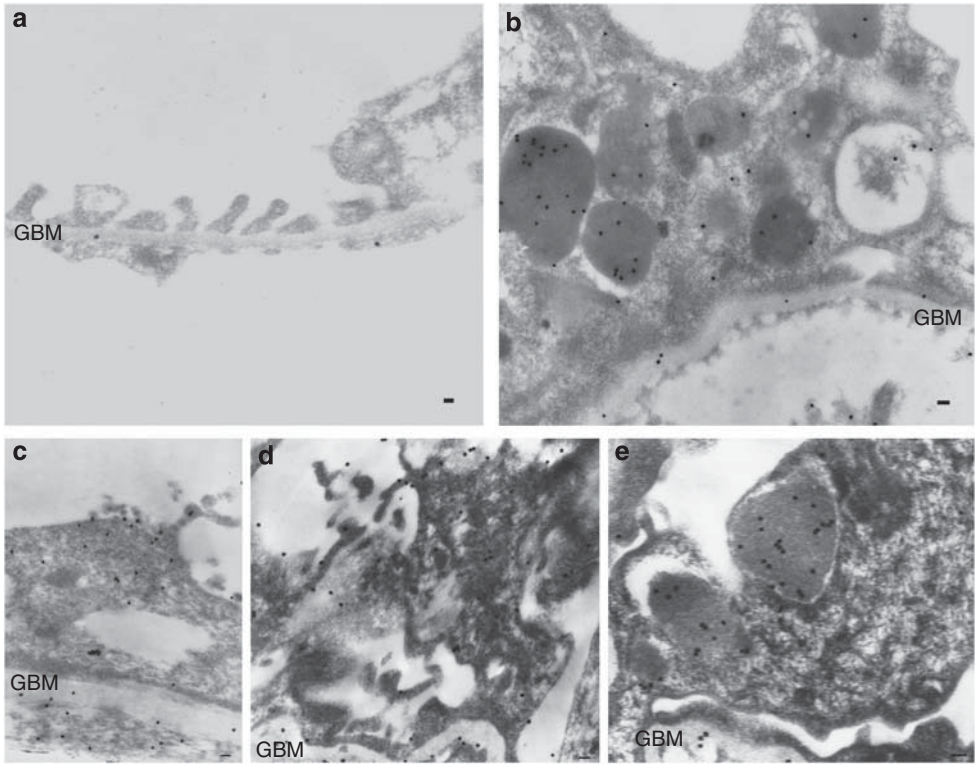

Figure 3 | Immunogold transmission electron microscopy (TEM) images labeling for Evans Blue-labeled human serum albumin in the podocytes. In the control (**a**), there were hardly any immunogold particles in podocytes. Many gold particles were present in podocyte vesicles (**b**), apical protrusions (**c**), microvilli (**d**), and vesicles just about to be excreted from the apical membrane (**e**) in puromycin aminonuculeoside (PAN) nephrotic rats. GBM, glomerular basement membrane. Bar = 100 nm.

we demonstrated by immunoprecipitation that human serum albumin bound to FcRn was increased in podocytes of PAN nephrotic rats, which decreased by apocynin treatment, suggesting that FcRn has a role in albumin transport (Figure 8a). To further confirm this, we treated PAN nephrotic rats with antibody against rat FcRn, which resulted in reduced proteinuria and suppressed uptake of EB-labeled human serum albumin in podocytes compared with untreated PAN nephrotic rats (Figure 8b–d).

DISCUSSION

The novel findings in this study are the presence of albumin endocytosis and excretion by podocytes in a MCNS animal model, and that the albumin receptor FcRn mediates this process. We have also shown that the NADPH oxidase inhibitor, apocynin, effectively suppressed this process and ameliorated proteinuria.

The most commonly accepted hypothesis of proteinuria in MCNS is that proteins leak from the slit pores with reduced nephrin expression.[19,20] However, it seems difficult to explain both massive proteinuria and selective albuminuria by reduction of nephrin leading to enlarged slit pores. Actually, in rats with a heterozygous defect in the nephrin gene, proteinuria was absent.[21] In addition, in nephrosis induced by nephrin antibodies, nephrin expression was lowest after 1 h, before proteinuria appeared, and proteinuria decreased at 2 weeks, when nephrin expression remained suppressed.[22,23] These findings raise doubts as to whether nephrin deficiency is a cause of proteinuria. It is possible that reduced nephrin expression in nephrotic syndromes is merely a reflection of the decrease in slit number.[24,25] Loss of the charge barrier is another hypothesis, but previous studies have shown that this alone is not sufficient to cause nephrosis.[5,26] Podocyte detachment or GBM rupturing causes nonselective proteinuria,[27,28] but they are usually absent in human MCNS and low-dose PAN nephrosis used in the present study. Thus, previous theories do not decisively explain the pathophysiology of selective proteinuria in MCNS.

We have confirmed in this study that PAN nephrosis presents with selective proteinuria; the selectivity of proteinuria evaluated by the urinary IgG/albumin ratio was comparable between PAN nephrotic rats and controls (Figure 2c and d). We made use of EB-labeled human serum albumin as a tracer to elucidate the mechanism of selective albuminuria, and results indeed suggested enhanced albumin endocytosis in nephrotic podocytes. Podocyte vesicles have often been observed in TEM studies of nephrotic syndrome kidneys, but their significance has been unclear.[29–33] Our immunogold TEM and SEM studies demonstrated that labeled albumin was taken up in these vesicles (Figures 3b and 4d). Considerable heterogeneity was observed among podocytes in the degree of human serum albumin uptake in

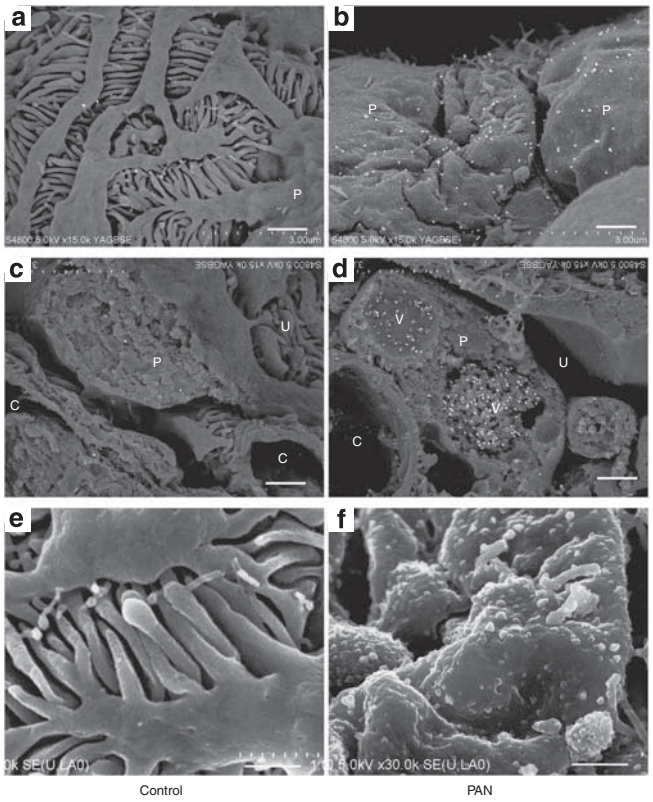

Figure 4 | Podocyte albumin transport as visualized by immunogold scanning electron microscope (SEM). (**a**–**d**) Immunogold SEM against human serum albumin after 90 min of injection in controls (**a**, **c**) and puromycin aminonucleoside (PAN) nephrotic rats (**b**, **d**). Many gold particles are present in cytoplasmic vesicles and on the cell surface of podocytes in PAN nephrotic rats. (**e**, **f**) Secondary electron images of the podocyte surface at high magnification. Many granular protrusions are seen on the podocyte surface in PAN nephrotic rats (**f**), whereas these are absent in controls (**e**). C, glomerular capillary; P, podocyte; U, urinary space; V, vesicle. Each group includes four rats. Bars = 1 μm (**a**–**d**), 500 nm (**e**, **f**).

PAN nephrotic rats, which is also proven by the large standard error value of the number of immunogold particles for EB-labeled human albumin in Figure 6g. However, this is consistent with a recent report that demonstrates focally high permeability for proteins around some podocytes in the PAN nephrotic model.[34] Recently, Eyre *et al.*[35] demonstrated that albumin is taken up in endosomes of cultured human podocytes. Uptake was specific for albumin, suggesting a receptor-mediated process. In addition, a SEM study observing the podocyte basolateral membrane, after removal of the GBM, revealed markedly increased coated pits in PAN nephrosis, suggesting enhanced endocytosis.[36] In our study, many albumin molecules were observed on the podocyte apical surface in PAN nephrosis by immunogold SEM (Figure 4b), implying excretion from the apical membrane. Numerous protrusions resembling shedding vesicles were observed in the SE mode (Figure 4f), which is consistent with the excretory pathway recently demonstrated in the kidney.[37,38] Thus, we hypothesized that podocytes may transport albumin by means of endocytosis and excretion by shedding in PAN rats.

Can podocytes actually transport such massive amounts of albumin? In the study by Eyre *et al.*,[35] the maximal rate of endocytosis was shown to be 97.4 μg/mg cell protein/h. Human glomeruli contain 878 ± 220 podocytes,[39] a human kidney contains approximately 10^6 glomeruli, and protein accounts for 21% of the total cell weight; thus, if the podocyte is represented as a sphere with a radius of 10 μm, the estimated total endocytic capacity in human kidneys will be 3.6 g/day [97.4 μg/mg cell protein/h × 0.21 mg cell protein/mg cell × $\frac{4}{3}\pi \times (10\,\mu m)^3$ × 878 cells per glomerulus × 2×10^6 glomeruli per kidney × 24 h]. This indicates that podocytes are capable of transporting nephrotic levels of protein, at least *in vitro*.

The mechanism of albumin-specific endocytosis has been established in other epithelial and endothelial cells, mediated by receptors such as megalin and gp60.[40–42] We have demonstrated that there is a marked increase in FcRn binding of albumin in podocytes of PAN nephrotic rats (Figure 8a), and treatment with an antibody against FcRn partially inhibited proteinuria and podocyte albumin uptake in the PAN nephrotic rats. FcRn may mediate podocyte albumin transport in MCNS, which may be the mechanism underlying selective albuminuria in this disease. The true roles of FcRn in podocytes are yet to be ascertained, and further studies are necessary.

A further important finding in our study is that it took more than 5 min after injection of labeled albumin before it is steadily excreted into the proximal tubular lumen (Figure 7a). This indicates that increased albumin excretion in MCNS is not mainly due to slit diaphragm dysfunction, because, if it is so, albumin filtration should be maximal soon after injection when plasma concentration is highest. This initial delay in excretion may reflect a period when albumin is transported through podocytes by endocytosis and shedding excretion.

The mechanism of podocyte dysfunction in PAN nephrosis is not understood in detail, but ROS overproduction is said to cause cytoskeletal changes such as actin disaggregation, resulting in foot process effacement and podocyte deformity.[43] We have shown that NADPH oxidase expression and superoxide production were increased in podocytes in PAN nephrosis before proteinuria appeared (Figure 5), suggesting that ROS may be a trigger leading to podocyte deformity and enhanced endocytosis. We have previously demonstrated that apocynin inhibits NADPH oxidase by preventing assembly of the p47phox and p67phox subunits within the membrane NADPH oxidase complex, and reduces albuminuria in diabetic nephropathy.[44] In this study, apocynin reduced podocyte superoxide production, partially restored foot processes, suppressed endocytosis via FcRn and shedding excretion of EB-labeled human serum albumin in podocytes, and reduced proteinuria (Figure 2, 5, 6). Increased podocyte vesicles containing albumin have also been observed in diabetic rats, and apocynin has been reported to

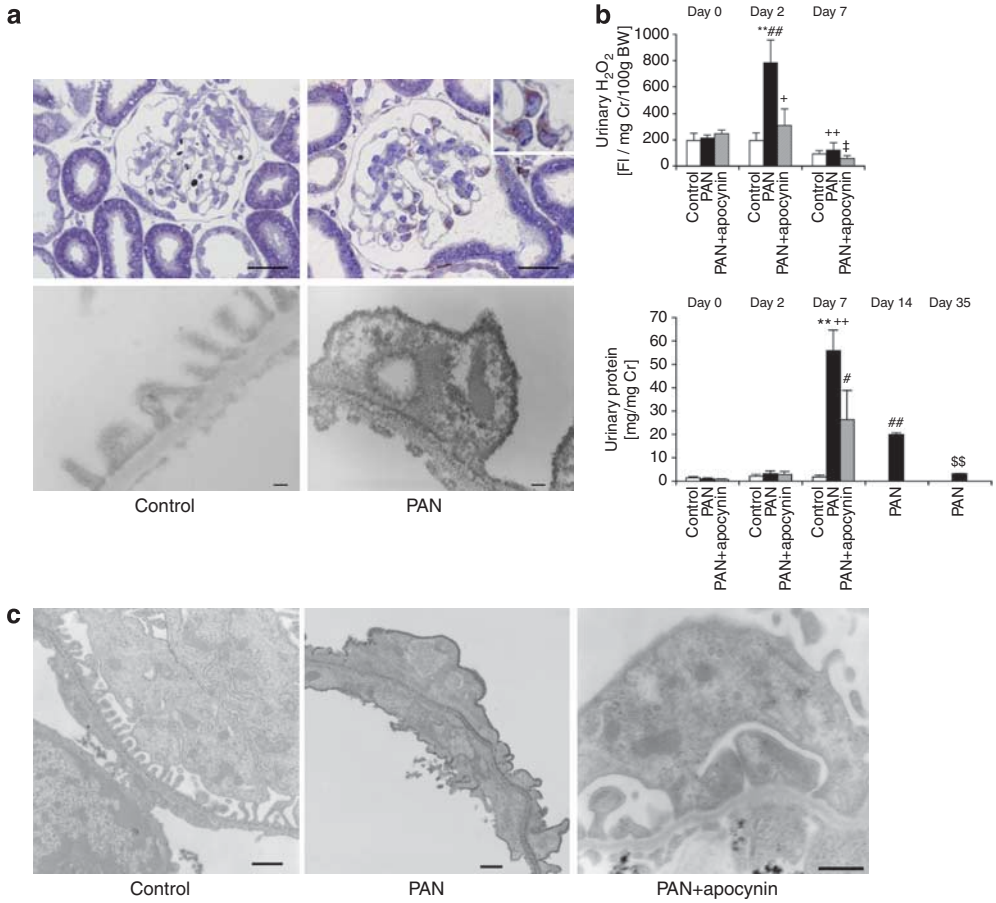

Figure 5 | Reactive oxygen species (ROS) production by NADPH oxidase in controls, puromycin aminonucleoside (PAN) nephrotic rats, and PAN rats treated with apocynin (PAN + apocynin). (**a**) Light micrographs (top, toluidine blue staining) and electron micrographs (bottom) of Lowicryl sections prepared for pre-embedding immunoelectron microscopy for the NADPH oxidase subunit p47phox. The inset shows an enlargement of the podocytes stained for p47phox. (**b**) Measurement of urinary hydrogen peroxide (H_2O_2) levels and proteinuria. $^{**}P<0.01$ versus control; $^{+}P<0.05$, $^{++}P<0.01$ versus PAN-2d; $^{\#}P<0.05$, $^{\#\#}P<0.01$ versus PAN-7d, $^{\$\$}P<0.01$ versus PAN-7d, $^{\ddagger}P<0.05$ versus PAN + apocynin. (**c**) Detection of ROS by cerium chloride histochemistry. Cerium chloride precipitation indicating superoxide production was observed on the plasma membrane of podocytes, the glomerular basement membrane, and endothelial cells on day 2 after puromycin injection in PAN nephrotic rats, which decreased with treatment by apocynin. Each group includes four to eight rats. Bars = 50 μm (**a**, top), 200 nm (**a**, bottom), and 500 nm (**c**). BW, body weight; Cr, creatinine.

reduce podocyte ROS and proteinuria in this condition.[30,44] On the basis of these observations, apocynin may inhibit albumin endocytosis in podocytes and may be a promising potential therapeutic drug for diseases presenting with selective proteinuria.

The limitations of this study are that we could not use two-photon excitation microscopy, which enables higher-quality imaging, and that we could not observe the glomerulus directly. However, our observation is consistent with the results of Russo *et al.*,[45] which visualize glomerular transport of Alexa 568-labeled albumin using two-photon microscopy. They demonstrated that labeled albumin was observed weakly in the proximal tubular lumen 40 s after injection and increased after 14 min in PAN nephrotic rats. As it is difficult to remove free Alexa 568 (MW 792) completely even by dialysis, fluorescence at 40 s may have been caused by free Alexa 568 filtered through the slit diaphragm. It is also possible that albumin uptake by podocytes may not be a main mechanism of albuminuria in MCNS, but a side phenomenon occurring in the podocytes surrounded by abundant protein in Bowman's space. Even if this is true, it is still important because albumin uptaken by podocytes may cause increased ROS production and podocyte damage, resulting in podocyte loss or apoptosis, and lead to massive proteinuria.[46,47] Finally, in this study, apocynin was administrated preventively, and therefore we have not verified whether the drug possesses a therapeutic effect when given after the onset of nephrotic syndrome.

In conclusion, EB-labeled human albumin was filtered only in trace amounts in controls, whereas in the minimal change nephrotic syndrome model, enhanced podocyte endocytosis of labeled albumin, mediated by FcRn, and excretion from the podocyte cell surface was observed, which resulted in selective albuminuria.

ROS overproduction by NADPH oxidase has a role in the disease pathogenesis, and inhibition with apocynin suppressed podocyte albumin endocytosis and excretion, and ameliorated proteinuria, shedding light on apocynin as a new therapeutic approach.

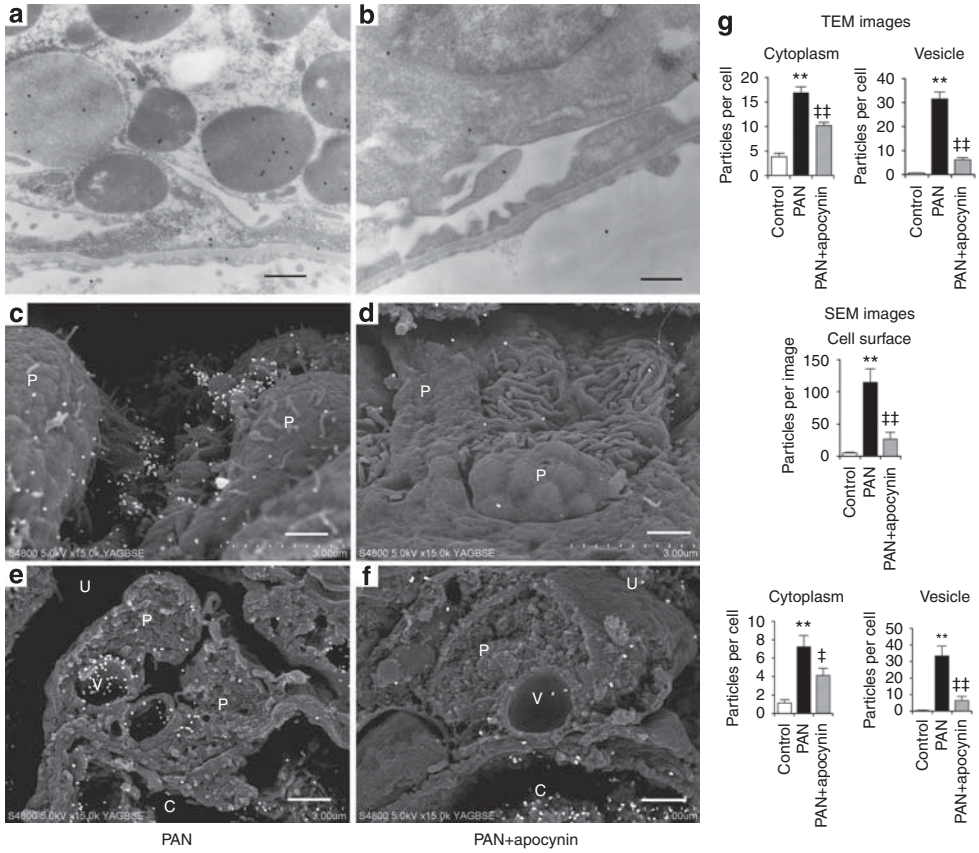

Figure 6 | Effect of apocynin on endocytosis and excretion of Evans Blue (EB)-labeled human serum albumin. (**a**–**f**) Observation by immunogold transmission electron microscopy (TEM) (**a**, **b**) and scanning electron microscope (SEM) (**c**–**f**) methods in puromycin aminonucleoside (PAN) nephrotic rats untreated ($n = 8$, **a**, **c**, **e**), or treated with apocynin (PAN + apocynin, $n = 5$, **b**, **d**, **f**) on day 5 after disease induction. C, glomerular capillary; P, podocyte; U, urinary space; V, vesicle. (**g**) Comparison of the number of immunogold particles labeling for EB-labeled human serum albumin within the podocyte cytoplasm, podocyte vesicles, and on the surface of podocytes in electron micrographs. A total of 30–50 images from kidney samples of three rats in each group were analyzed. $^{**}P < 0.01$ versus control. $^{‡}P < 0.05$, $^{‡‡}P < 0.01$ versus PAN. Bars = 500 nm (**a**, **b**) and 1 μm (**c**–**f**).

MATERIALS AND METHODS

Animals and experimental designs

Male Sprague–Dawley rats (Charles River Laboratories, Shizuoka, Japan) weighing 110–130 g, housed in a temperature- and humidity-controlled room with access to tap water and standard animal chow, were used as controls ($n = 11$), and nephrotic syndrome was induced by intraperitoneal administration of PAN (15 mg/100 g body weight; Sigma Chemical, St Louis, MO, $n = 17$). Five days later, nephrotic syndrome was confirmed by measurement of urinary protein. For *in vivo* confocal microscopy, GFP transgenic rats (Lewis transgenic rats; a generous gift from PhoenixBio, Tochigi, Japan) that ubiquitously express enhanced GFP were used.[48] Some PAN nephrotic rats were continuously treated with apocynin (4-hydroxy-3-methoxyacetophenone, 16 mg/kg/day in drinking water; Avocado Research Chemicals, Heysham, UK, $n = 8$), starting 2 days before PAN administration. As described later, six male Sprague–Dawley rats weighing 60–100 g were used for the study of the treatment with antibody against rat FcRn. Animals were anesthetized with pentobarbital (50 mg/kg body weight). All procedures were conducted in accordance with the Guide for Animal Experimentation of the Faculty of Medicine, The University of Tokyo (Tokyo, Japan), and the NIH Guide for the Care and Use of Laboratory Animals. This study has been approved by the Medical Experimental Animal Ethics Committee of the University of Tokyo (approval number P10-079).

Glomerular transport of EB-labeled human serum albumin

EB was added to 4% human serum albumin in sterile physiological saline at a 3:1 molecular ratio. EB-labeled human serum albumin was continuously infused at 1 ml/h for 90 min following 1 ml injection through a jugular vein catheter. Kidneys were fixed with either 2.5% glutaraldehyde and 2% paraformaldehyde in 0.01 M phosphate-buffered saline or periodate-lysine-paraformaldehyde solution and embedded in epoxy resin and Lowicryl (Electron Microscopy Sciences, Washington, PA), respectively. Slices (100 μm) cut by vibratome (Dosaka EM, Kyoto, Japan) were observed by light microscopy. Lowicryl sections (5 μm) were also observed with excitation at 568 nm, laser power at 30 mW, and 599 ms exposure time to detect EB fluorescence in podocytes.

In vivo visualization of podocyte EB-labeled human serum albumin uptake and excretion by confocal microscopy

Two GFP rats in which PAN nephrosis was induced and one control GFP rat were anesthetized, then the left kidney was placed in a kidney cup, and observed under a real-time confocal scanner unit CSU-21 (Yokogawa Electric Corporation, Tokyo, Japan). After

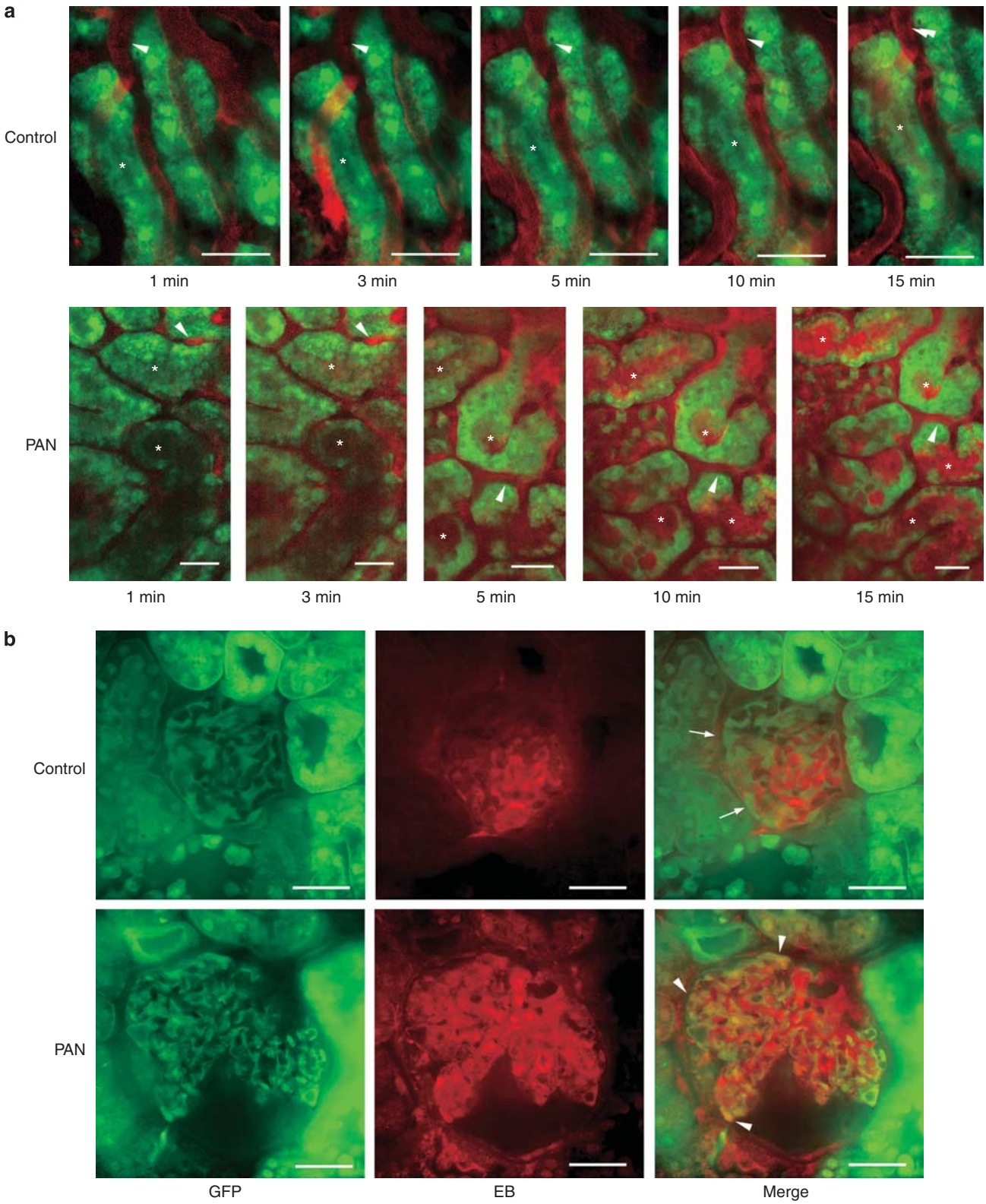

Figure 7 | Renal handling of Evans Blue (EB)-labeled human serum albumin in green fluorescent protein (GFP) transgenic rats. (**a**) Real-time confocal microscopic images of the renal tubules after injection of EB-labeled human serum albumin in puromycin aminonucleoside (PAN) nephrotic GFP transgenic rats and their controls. EB fluorescence appeared immediately in the peritubular capillaries (arrowheads), and later in the tubular lumen (indicated by asterisks) after 5 min in PAN rats, but not in the control. (**b**) Confocal microscopic images of glomeruli in vibratome sections. Podocytes uptaking EB-labeled human serum albumin turned yellow (arrowheads) in PAN nephrotic rats, whereas podocytes without EB-labeled human serum albumin endocytosis showed GFP fluorescence in controls (arrows). The degree of podocyte EB-labeled human serum albumin uptake was heterogenous among cells. Bar = 50 μm.

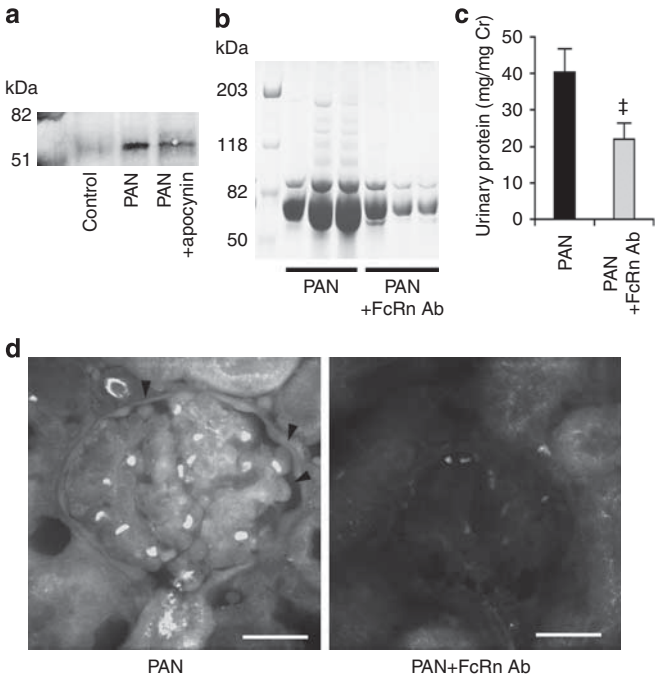

Figure 8 | Role of FcRn as an albumin receptor in the podocyte. (**a**) Immunoprecipitation analysis of isolated glomeruli with anti-FcRn antibody. (**b**) SDS-PAGE of urinary protein from puromycin aminonucleoside (PAN) nephrotic rats ($n = 3$) and PAN nephrotic rats treated with antibody against rat FcRn (PAN + FcRn Ab, $n = 3$) at day 5. (**c**) Amount of urinary protein per mg creatinine. $^{\ddagger}P < 0.05$ versus PAN. (**d**) Confocal microscopic images of glomeruli in Lowicryl sections after 15 min of Evans Blue-labeled human serum albumin. Podocytes are marked by arrowheads. Bar = 50 μm.

intravenous injection of 0.5 ml 4% human serum albumin bound to EB at a 3:1 molecular ratio, real-time confocal images of fluorescence for GFP (emission peak at 509 nm) and EB (emission peak at 680 nm) were taken at 0, 1, 3, 5, 10, and 15 mins. All images for EB fluorescence were taken with excitation at 568 nm, laser power at 20 mW, and 1.56 s exposure time, whereas the settings for all GFP fluorescence images were excitation at 488 nm, laser power at 20 mW, and exposure time for 599 ms. A total of 30 images were taken with 0.36 s intervals for each time point, and well-focused images were chosen and overlayed to create the final image. After 15 min, vibratome slices of the kidney were observed by confocal microscopy to detect EB fluorescence in podocytes.

Measurement of urine and serum EB-labeled human serum albumin, protein, and creatinine

Blood and urine samples were collected before and after bolus injection of 2 ml EB-labeled human serum albumin, using metabolic cages. The concentration of EB-labeled human serum albumin was measured by fluorescent spectrophotometry (Hitachi F-2000, Tokyo, Japan) with excitation and emission wavelengths of 540 and 680 nm, respectively. Protein and creatinine concentrations were measured by spectrophotometry as described previously.[44]

Western blot for human serum albumin of isolated glomeruli and SDS-PAGE of urine

After infusion of EB-labeled human serum albumin, 200 glomeruli were isolated by graded sieving of the kidney and microdissection, and western blotting was performed with rabbit anti-human serum albumin antibody (Dako, Glostrup, Denmark) as the primary antibody and HRP-conjugated anti-rabbit immunoglobulin (Dako) as the secondary antibody, both at 1:400 dilution as described previously.[49] We also performed SDS-PAGE for urine from five rats in each group. The area and density of bands for albumin and IgG were measured using the NIH image software, and urinary protein selectivity was evaluated by the urinary IgG/albumin ratio.

Immunoprecipitation of glomerular proteins with anti-FcRn antibody

The homogenate solution of 200 isolated glomeruli per rat was incubated with protein A-sepharose for 30 min to remove nonspecific precipitation. After centrifugation at 15,000 r.p.m. for 5 s, the supernatant was incubated for 2 h at 4 °C with the addition of a goat anti-FcRn antibody (Santa Cruz Biotechnology, Santa Cruz, CA) at 1:25 dilution and 10 μl protein A-sepharose. After repeated washing by re-suspending in 4 °C lysis buffer and centrifuging at 2000*g* for 2 min, 20 μl sample buffer was added. Samples were subjected to SDS-PAGE, and western blotting was performed with rabbit anti-human serum albumin antibody at 1:200 dilution, followed by HRP-conjugated secondary antibody at 1:200 dilution and 3,3' diaminobenzidine staining.

Administration of anti-FcRn antibody to PAN nephrotic rats

PAN nephrotic syndrome was induced in six male Sprague–Dawley rats weighing 60–100 g, and in three rats, 200–400 μg of anti-rat FcRn antibody (Santa Cruz Biotechnology) was intraperitoneally administered on the same day as PAN was induced. Urine was collected for 8 h, and protein and creatinine concentrations were measured, and SDS-PAGE of urine collected on day 5 after PAN administration was performed. Subsequently, 1 ml of EB-labeled human serum albumin was intravenously injected, and after 15 min, kidneys were fixed with periodate-lysine-paraformaldehyde solution and the sections were observed with a confocal microscope.

Immunogold TEM and SEM

Immunogold TEM specimens were prepared as described previously.[50] Briefly, ultrathin sections of Lowicryl blocks were incubated with rabbit polyclonal antibody against human serum albumin (Dako Glostrup) at 1:50 dilution, and then with 25-nm gold-labeled goat anti-rabbit IgG antibody (Aurion, Wageningen, the Netherlands) at 1:50 dilution for 4 h, and examined by TEM (Hitachi H-7000). We counted the number of immunogold particles observed within the podocyte cytoplasm and podocyte vesicles in 30–50 micrographs from each group (magnification × 15,000).

For immunogold SEM, as described previously,[51] periodate-lysine-paraformaldehyde-fixed kidneys were cut by vibratome into 150-μm slices, and incubated with rabbit anti-human serum albumin antibody as the primary antibody and 25 nm gold-labeled goat anti-rabbit IgG antibody as the secondary antibody. After silver enhancement (Aurion), samples were osmium coated at a thickness of 5 nm with an osmium plasma coater (Filgen, Nagoya, Japan), and observed by SEM (Hitachi S-4800) by backscattered electron imaging. The number of gold particles within the podocyte cytoplasm and podocyte vesicles, as well as on the surface of podocytes, was compared at × 15,000 magnification.

Cerium chloride histochemistry and urinary H_2O_2 measurement

We performed cerium chloride histochemistry by the methods of Schlafer *et al.*[52] Briefly, the abdominal aorta was cannulated, and kidneys were perfused retrogradely for 10 min with 100 ml 1 mmol/l cerium chloride in imidazole-buffered physiological saline solution (143 mmol/l NaCl, 4 mmol/l KCl, 25 mmol/l $NaHCO_3$, 1.2 mmol/l $MgCl_2$, 2.4 mmol/l $CaCl_2$, 11 mmol/l glucose; 37 °C, pH 7.4). Kidneys were fixed with 2.5% glutaraldehyde and 2% paraformaldehyde in 0.01 M phosphate-buffered saline and embedded in epoxy resin. Ultrathin sections were examined by TEM. Urinary H_2O_2 was measured before PAN injection and at days 2 and 7 as described previously.[53]

Pre-embedding immunoelectron microscopy for p47phox

To detect the NADPH oxidase component p47phox, pre-embedding immunoelectron microscopy was performed as described previously.[54] Briefly, 50 µm vibratome sections were incubated overnight with polyclonal anti-p47phox antibodies (Santa Cruz Biotechnology) at 1:100 dilution, and then incubated for 1 h with HRP-conjugated anti-rabbit IgG secondary antibody at 1:50 dilution. HRP signals were developed by 3,3' diaminobenzidine, and ultrathin sections were observed by TEM.

Statistics

All data are shown as mean ± s.e.m. Mean values were compared among groups using analysis of variance, followed, where appropriate, by Fisher's protected least significant difference test as a *post hoc* test. *P*-values <0.05 were considered to be significant.

DISCLOSURE

All the authors declared no competing interests.

ACKNOWLEDGMENTS

This work is partly supported by a grant-in-aid for scientific research from Japan Science Promotion Foundation to AT (C-19590938).

REFERENCES

1. Deen WM, Lazzara MJ, Myers BD. Structural determinants of glomerular permeability. *Am J Physiol Renal Physiol* 2001; **281**: F579–F596.
2. Yamada E. The fine structure of the renal glomerulus of the mouse. *J Biophys Biochem Cytol* 1955; **1**: 551–566.
3. Farquhar MG, Wissig SL, Palade GE. Glomerular permeability. I. Ferritin transfer across the normal glomerular capillary wall. *J Exp Med* 1961; **113**: 47–66.
4. Caulfield JP, Farquhar MG. The permeability of glomerular capillaries to graded dextrans. Identification of the basement membrane as the primary filtration barrier. *J Cell Biol* 1974; **63**: 883–903.
5. Brenner BM, Hostetter TH, Humes HD. Glomerular permselectivity: barrier function based on discrimination of molecular size and charge. *Am J Physiol* 1978; **234**: F455–F460.
6. Jarad G, Cunningham J, Shaw AS *et al.* Proteinuria precedes podocyte abnormalities in Lamb2−/− mice, implicating the glomerular basement membrane as an albumin barrier. *J Clin Invest* 2006; **116**: 2272–2279.
7. Rodewald R, Karnovsky MJ. Porous substructure of the glomerular slit diaphragm in the rat and mouse. *J Cell Biol* 1974; **60**: 423–433.
8. Venkatachalam MA, Karnovsky MJ, Cotran RS. Glomerular permeability—ultrastructural studies in experimental nephrosis using horseradish peroxidase as a tracer. *J Exp Med* 1969; **130**: 381–399.
9. Venkatachalam MA, Cotran RS, Karnovsky MJ. An ultrastructural study of glomerular permeability in aminonucleoside nephrosis using catalase as a tracer protein. *J Exp Med* 1970; **132**: 1168–1180.
10. Tryggvason K. Unraveling the mechanisms of glomerular ultrafiltration: nephrin, a key component of the slit diaphragm. *J Am Soc Nephrol* 1999; **10**: 2440–2445.
11. Tryggvason K, Patrakka J, Wartiovaara J. Hereditary proteinuria syndromes and mechanisms of proteinuria. *N Engl J Med* 2006; **354**: 1387–1401.
12. Patrakka J, Lahdenkari AT, Koskimies O *et al.* The number of podocyte slit diaphragms is decreased in minimal change nephrotic syndrome. *Pediatr Res* 2002; **52**: 349–355.
13. Tojo A, Onozato ML, Kitiyakara C *et al.* Glomerular albumin filtration through podocyte cell body in puromycin aminonucleoside nephrotic rat. *Med Mol Morphol* 2008; **41**: 92–98.
14. Stopa B, Rybarska J, Drozd A *et al.* Albumin binds self-assembling dyes as specific polymolecular ligands. *Int J Biol Macromol* 2006; **40**: 1–8.
15. Tojo A, Asaba K, Onozato ML. Suppressing renal NADPH oxidase to treat diabetic nephropathy. *Expert Opin Ther Targets* 2007; **11**: 1011–1018.
16. Haymann JP, Levraud JP, Bouet S *et al.* Characterization and localization of the neonatal Fc receptor in adult human kidney. *J Am Soc Nephrol* 2000; **11**: 632–639.
17. Akilesh S, Huber TB, Wu H *et al.* Podocytes use FcRn to clear IgG from the glomerular basement membrane. *Proc Natl Acad Sci U S A* 2008; **105**: 967–972.
18. Conway-Jacobs A, Lewin LM. Isoelectric focusing in acrylamide gels: use of amphoteric dyes as internal markers for determination of isoelectric points. *Anal Biochem* 1971; **43**: 394–400.
19. Lahdenkari AT, Lounatmaa K, Patrakka J *et al.* Podocytes are firmly attached to glomerular basement membrane in kidneys with heavy proteinuria. *J Am Soc Nephrol* 2004; **15**: 2611–2618.
20. Pricam C, Humbert F, Perrelet A *et al.* Intercellular junctions in podocytes of the nephrotic glomerulus as seen with freeze-fracture. *Lab Invest* 1975; **33**: 209–218.
21. Putaala H, Soininen R, Kilpelainen P *et al.* The murine nephrin gene is specifically expressed in kidney, brain and pancreas: inactivation of the gene leads to massive proteinuria and neonatal death. *Hum Mol Genet* 2001; **10**: 1–8.
22. Orikasa M, Matsui K, Oite T *et al.* Massive proteinuria induced in rats by a single intravenous injection of a monoclonal antibody. *J Immunol* 1988; **141**: 807–814.
23. Kawachi H, Koike H, Kurihara H *et al.* Cloning of rat nephrin: expression in developing glomeruli and in proteinuric states. *Kidney Int* 2000; **57**: 1949–1961.
24. Langham RG, Kelly DJ, Cox AJ *et al.* Proteinuria and the expression of the podocyte slit diaphragm protein, nephrin, in diabetic nephropathy: effects of angiotensin converting enzyme inhibition. *Diabetologia* 2002; **45**: 1572–1576.
25. Duner F, Lindstrom K, Hultenby K *et al.* Permeability, ultrastructural changes, and distribution of novel proteins in the glomerular barrier in early puromycin aminonucleoside nephrosis. *Nephron Exp Nephrol* 2010; **116**: E42–E52.
26. Rossi M, Morita H, Sormunen R *et al.* Heparan sulfate chains of perlecan are indispensable in the lens capsule but not in the kidney. *EMBO J* 2003; **22**: 236–245.
27. Whiteside C, Prutis K, Cameron R *et al.* Glomerular epithelial detachment, not reduced charge density, correlates with proteinuria in adriamycin and puromycin nephrosis. *Lab Invest* 1989; **61**: 650–660.
28. Ota Z, Ota K, Ota S *et al.* Dynamic analysis on rupture of glomerular basement membranes in glomerulonephritis. *Nephron* 1998; **79**: 345–347.
29. Rastaldi MP, Armelloni S, Berra S *et al.* Glomerular podocytes contain neuron-like functional synaptic vesicles. *FASEB J* 2006; **20**: 976–978.
30. Nishiyama A, Nakagawa T, Kobori H *et al.* Strict angiotensin blockade prevents the augmentation of intrarenal angiotensin II and podocyte abnormalities in type 2 diabetic rats with microalbuminuria. *J Hypertens* 2008; **26**: 1849–1859.
31. Rollason TP, Brewer DB. A scanning and transmission electron microscopic study of glomerular damage in the rat following heterologous serum albumin overload. *J Pathol* 1981; **134**: 39–56.
32. Gross ML, Ritz E, Schoof A *et al.* Comparison of renal morphology in the Streptozotocin and the SHR/N-cp models of diabetes. *Lab Invest* 2004; **84**: 452–464.
33. Kerjaschki D. Dysfunctions of cell biological mechanisms of visceral epithelial cell (podocytes) in glomerular diseases. *Kidney Int* 1994; **45**: 300–313.
34. Peti-Peterdi J, Sipos A. A high-powered view of the filtration barrier. *J Am Soc Nephrol* 2010; **21**: 1835–1841.
35. Eyre J, Ioannou K, Grubb BD *et al.* Statin-sensitive endocytosis of albumin by glomerular podocytes. *Am J Physiol Renal Physiol* 2007; **292**: F674–F681.
36. Inokuchi S, Shirato I, Kobayashi N *et al.* Re-evaluation of foot process effacement in acute puromycin aminonucleoside nephrosis. *Kidney Int* 1996; **50**: 1278–1287.
37. Hara M, Yanagihara T, Hirayama Y *et al.* Podocyte membrane vesicles in urine originate from tip vesiculation of podocyte microvilli. *Hum Pathol* 2010; **41**: 1265–1275.

38. Hara M, Yanagihara T, Kihara I *et al.* Apical cell membranes are shed into urine from injured podocytes: a novel phenomenon of podocyte injury. *J Am Soc Nephrol* 2005; **16**: 408–416.
39. Steffes MW, Schmidt D, McCrery R *et al.* Glomerular cell number in normal subjects and in type 1 diabetic patients. *Kidney Int* 2001; **59**: 2104–2113.
40. Johnson LG, Cheng PW, Boucher RC. Albumin absorption by canine bronchial epithelium. *J Appl Physiol* 1989; **66**: 2772–2777.
41. Christensen EI, Birn H. Megalin and cubilin: multifunctional endocytic receptors. *Nat Rev Mol Cell Biol* 2002; **3**: 256–266.
42. Tojo A, Onozato ML, Ha H *et al.* Reduced albumin reabsorption in the proximal tubule of early-stage diabetic rats. *Histochem Cell Biol* 2001; **116**: 269–276.
43. Diamond JR, Bonventre JV, Karnovsky MJ. A role for oxygen free radicals in aminonucleoside nephrosis. *Kidney Int* 1986; **29**: 478–483.
44. Asaba K, Tojo A, Onozato ML *et al.* Effects of NADPH oxidase inhibitor in diabetic nephropathy. *Kidney Int* 2005; **67**: 1890–1898.
45. Russo LM, Sandoval RM, McKee M *et al.* The normal kidney filters nephrotic levels of albumin retrieved by proximal tubule cells: retrieval is disrupted in nephrotic states. *Kidney Int* 2007; **71**: 504–513.
46. Gu L, Hagiwara S, Fan Q *et al.* Role of receptor for advanced glycation end-products and signalling events in advanced glycation end-product-induced monocyte chemoattractant protein-1 expression in differentiated mouse podocytes. *Nephrol Dial Transplant* 2006; **21**: 299–313.
47. Cohen MP, Chen S, Ziyadeh FN *et al.* Evidence linking glycated albumin to altered glomerular nephrin and VEGF expression, proteinuria, and diabetic nephropathy. *Kidney Int* 2005; **68**: 1554–1561.
48. Inoue H, Ohsawa I, Murakami T *et al.* Development of new inbred transgenic strains of rats with LacZ or GFP. *Biochem Biophys Res Commun* 2005; **329**: 288–295.
49. Ookata K, Tojo A, Suzuki Y *et al.* Localization of inward rectifier potassium channel Kir7.1 in the basolateral membrane of distal nephron and collecting duct. *J Am Soc Nephrol* 2000; **11**: 1987–1994.
50. Tojo A, Welch WJ, Bremer V *et al.* Colocalization of demethylating enzymes and NOS and functional effects of methylarginines in rat kidney. *Kidney Int* 1997; **52**: 1593–1601.
51. Kinugasa S, Tojo A, Sakai T *et al.* Silver-enhanced immunogold scanning electron microscopy using vibratome sections of rat kidneys: detection of albumin filtration and reabsorption. *Med Mol Morphol* 2010; **43**: 218–225.
52. Shlafer M, Brosamer K, Forder JR *et al.* Cerium chloride as a histochemical marker of hydrogen peroxide in reperfused ischemic hearts. *J Mol Cell Cardiol* 1990; **22**: 83–97.
53. Onozato ML, Tojo A, Goto A *et al.* Oxidative stress and nitric oxide synthase in rat diabetic nephropathy: effects of ACEI and ARB. *Kidney Int* 2002; **61**: 186–194.
54. Tojo A, Onozato ML, Fukuda S *et al.* Nitric oxide generated by nNOS in the macula densa regulates the afferent arteriolar diameter in rat kidney. *Med Electron Microsc* 2004; **37**: 236–241.